

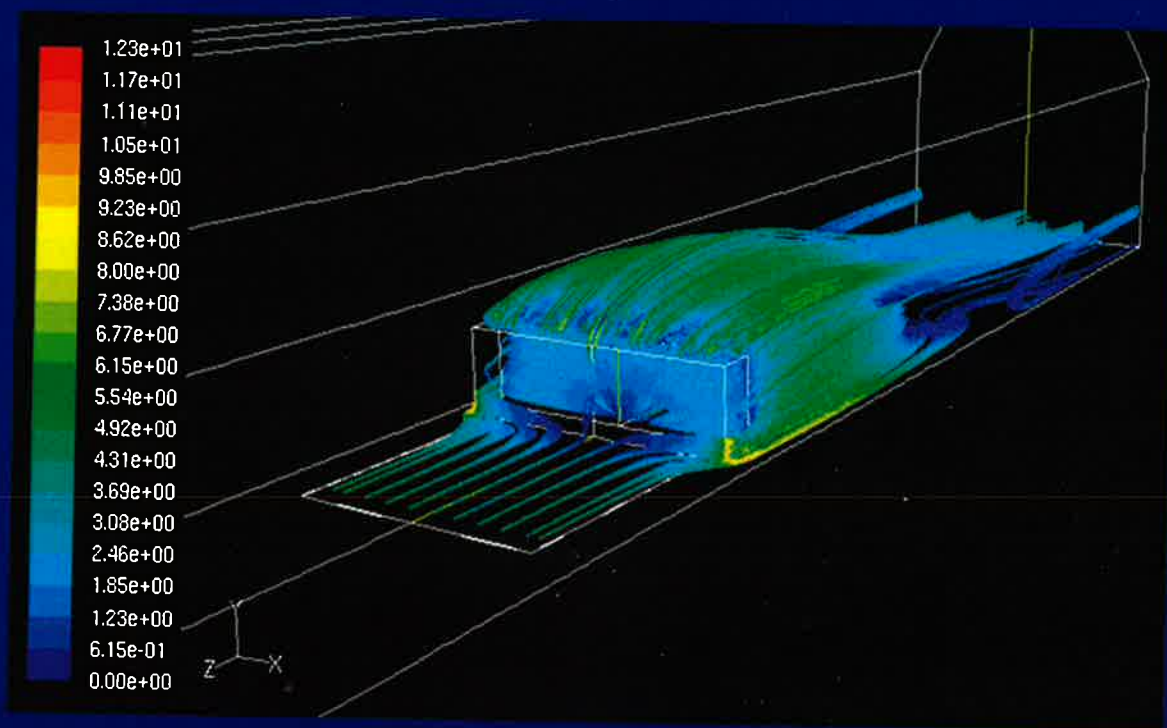
VOL. 107, NO. 4, OCTOBER 2014

HEALTH PHYSICS

THE RADIATION SAFETY JOURNAL



The Official Journal of
the Health Physics Society



www.health-physics.com



 Wolters Kluwer
Health

Lippincott
Williams & Wilkins

HEALTH PHYSICS

Offices, Subscriptions, Permission, and Publication Information

Health Physics (ISSN 0017-9078), a peer reviewed journal, is a publication of the Health Physics Society and is published monthly by Lippincott Williams & Wilkins, 16522 Hunters Green Parkway, Hagerstown, MD, 21740-2116. Business offices are located at Two Commerce Square, 2001 Market St., Philadelphia, PA 19103. Periodical postage paid at Hagerstown, MD, and at additional mailing offices. Copyright © 2014 by the Health Physics Society.

Health Physics Society Office: Mr. Brett Burk, Executive Director, Health Physics Society, 1313 Dolley Madison Boulevard, Suite 402, McLean, VA 22101. Tel. 703.790.1745. Member subscribers should inform the Executive Director of changes of address 90 days in advance. Membership dues: Please see the Prospectus in the back of this issue; application for membership should be made to the Executive Director of the Health Physics Society.

Health Physics Editorial Office: Mary Gene Ryan, Managing Editor, Health Physics, Editorial Office, 318 Island Park Dr., Charleston, SC 29492. Tel. 1.843.670.9668, E-mail journaloffice@burkinc.com. Author Guidelines will appear in the back of the January and July issues.

Publishing and Advertising: Lippincott Williams & Wilkins, 351 West Camden Street, Baltimore, MD 21201-2436. Tel. 1.800.882.0483 from anywhere in the U.S., Canada and Mexico. Outside North America, Tel. 1.410.528.4381, FAX 1.410.361.8016 or .8040. For information about advertising in the journal, Dee Bolognini at 646.674.6645 or faridih.bolognini@wolterskluwer.com.

Change of address for members: Member subscribers must notify the Health Physics Society Office of address changes. All other subscribers must notify the publisher 60 days in advance. Journals undeliverable because of incorrect address will be destroyed. Duplicate copies may be obtained, if available, from the Publisher at the regular price of a single issue. HPS members: Please send your changes of address to Brett Burk, Health Physics Society, 1313 Dolley Madison Boulevard, Suite 402, McLean, VA 22101; or log on to www.hps.org/membersonly/ and select "Directory." Thank you.

Address for nonmember subscription information, orders, or change of address: P. O. Box 1580, Hagerstown, MD 21741-1580; phone 1-800-638-3030 or 1-301-223-2300; fax 1-301-223-2400. In Japan, contact LWW Igaku-Shoin Ltd., 3-23-14 Hongo, Bunkyo-ku, Tokyo 113-0033; phone 81-3-5689-5400; fax 81-3-5689-5402. In Bangladesh, India, Nepal, Sri Lanka, and Pakistan, contact Globe Publications Pvt. Ltd. B-13 3rd Floor, A Block, Shopping Complex, Naraina Vihar, Ring Road, New Delhi, 110028; India phone 91-11-579-3211; fax 91-11-579-8876. **Bulk subscriptions:** For information on bulk subscription orders, please call Carol Bak at 1.410.528.4163.

Annual subscription rates: United States—\$709.00 Individual, \$2,842.00 Institution. *Rest of World*—\$771.00 Individual, \$2,934.00 Institution. Single copy rate \$237.00. Subscriptions outside the United States must be prepaid. Subscriptions outside North America must add \$32.00 for airfreight delivery. GST tax of 7% will be added to the subscription price of all orders shipped to Canada. (Lippincott Williams & Wilkins' GST Identification #895524239. Publications Mail Agreement #40052291). Prices subject to change without notice. Subscriptions will begin with currently available issue unless otherwise requested. Copies will be replaced without charge if the publisher receives a request within 90 days of the mailing date. Subscriptions should be renewed promptly to avoid a break in journal delivery. The publisher cannot guarantee to supply back issues on late renewals. Individual subscription rates include print and access to the online version. Institutional rates are for print only; online subscriptions are available via Ovid. Institutions can choose to purchase a print and online subscription together for a discounted rate. Institutions that wish to purchase a print subscription, please contact Lippincott Williams & Wilkins, 16522 Hunters Green Parkway, Hagerstown, MD 21740-2116; phone 800-638-3030 (outside the United States 301-223-2300); fax 301-223-2400. Institutions that wish to purchase an online subscription or online with print, please contact the Ovid Regional Sales Office near you or visit www.ovid.com/site/index.jsp and select Contact and Locations.

Back Issues: Back issues of all previously published volumes are available direct from Pergamon Press, Inc., 395 Saw Mill Road, Elmsford, NY 10523. Back issues beginning with Volume 74 are available from Lippincott Williams & Wilkins.

Reprints of individual articles are available from the authors or from the Institute for Scientific Information at 1.800.336.4474. Authors needing information on their reprint order may call 1.800.341.2258.

Reprints (non-author) in large quantities, for commercial or academic use, may be purchased from the Publisher. For information and prices call 1.800.358.3583, 410.528.8521 or E-mail Matt.Westcoat@wolterskluwer.com.

Permission to reproduce copies of articles for non-commercial use: This may be obtained from the Copyright Clearance Center, 222 Rosewood Drive, Danvers, MA 01923, 978.750.8400, FAX 978.750.4470, www.copyright.com.

Permission for other use: The copyright owner's consent does not extend to copying for general distribution, for promotion, for creating new works, or for resale. Specific written permission must be obtained from the publisher for such copying. Please contact the *Health Physics* Journal Editorial Office, 318 Island Park Dr., Charleston, SC 29492.

It is a condition of publication that manuscripts submitted to this journal have not been published and will not be simultaneously submitted or published elsewhere. By submitting a manuscript, the authors agree that the copyright for their article is transferred to the Health Physics Society if and when the article is accepted for publication. However, assignment of copyright is not required from authors who work for organizations that do not permit such assignment. The copyright covers the exclusive rights to reproduce and distribute the article, including reprints, photographic reproductions, microfilm, or any other reproduction of similar nature and translations. No part of this publication may be reproduced, stored in a retrieval system, or transmitted in any form or by any means—electronic, electrostatic, magnetic tape, mechanical photocopying, recording, or otherwise—without permission in writing from the copyright holder.

Disclaimer: Statements and opinions expressed in publications of the Health Physics Society or in presentations given during its regular meetings are those of the author(s) and do not necessarily reflect the official positions of the Health Physics Society, the editors, the publisher, or the organizations with which the authors are affiliated. The editor(s), publisher, and Society disclaim any responsibility or liability for such material and do not guarantee, warrant, or endorse any product or service mentioned. Official positions of the Society are established only by its Board of Directors.

Periodicals postage paid at Hagerstown, MD, and additional mailing offices.

Printed on acid-free paper.

Indexed in *Current Contents (Life Sciences, Science Citation Index, SciSearch Database, ISI/BioMed, Research Alert)*, *BIOSIS, Index Medicus, MEDLINE, Excerpta Medica, Chem. Abstr., WRC Info., Environ. Per. Bibl., Cancer Journals and Serials, Applied Health Phys. Abstr., Aqualine Abstr., Current Awareness in Biological Sciences, Energy Res. Abstr., Congress. Info. Serv. Index, ASSIA, Cambridge Scientific Service, PASCAL-CNRS Database, NISC's Fish and Fisheries Worldwide, and Energy Database.*

USING ISOTOPIC RATIOS FOR DISCRIMINATION OF ENVIRONMENTAL ANTHROPOGENIC RADIOACTIVITY

Robert B. Hayes and Mansour Akbarzadeh*

Abstract—When air is pulled into the WIPP repository for ventilation purposes, this air is unfiltered and contains all the components of ubiquitous anthropogenic radionuclides from global nuclear fallout (including ^{137}Cs and Pu isotopes). Although the NORM in aeolian sand and dust contribute to the gross alpha beta activity on effluent air filters, there remains a need to discriminate effluent TRU generated in the disposal process at WIPP from TRU being pulled into the repository with the unfiltered surface air. This is only evaluated using ratios of Cs and Pu activity found through radioassay of air filters taken from the mine effluent. By characterizing both the credible range of $^{137}\text{Cs}/^{239,240}\text{Pu}$ ratios from the environment and those known to exist in the waste, a rigorous test criteria is attained. The use of HPGE to assay ^{137}Cs in the intake dust plated out in the mine allowed a gross assay of total TRU radioactivity pulled into the mine over time from global fallout. Radiochemistry of samples from deposition in the mine's air intake shaft was also carried out. The use of net activity ratios at background levels is also shown to follow a Cauchy distribution in terms of their expected statistical distributions.

Health Phys. 107(4):277–291; 2014

Key words: aerosols; air sampling; modeling, environmental; waste management

INTRODUCTION

THE WASTE Isolation Pilot Plant (WIPP) is located in the southeast corner of New Mexico. The site is composed of various surface facilities supporting an underground salt mine located approximately 655 m underground. The WIPP mission includes disposing of plutonium-contaminated waste materials in a deep geological medium to permanently remove them from the biosphere. The facility prides itself on substantial operational throughput while maintaining the highest standards in safety, quality, and regulatory compliance.

*Nuclear Waste Partnership, WIPP Site, Carlsbad, NM 88220.

The authors declare no conflicts of interest.

For correspondence contact: Robert Hayes at the above address, or email at robert.hayes@wipp.ws.

(Manuscript accepted 30 January 2014)

0017-9078/14/0

Copyright © 2014 Health Physics Society

DOI: 10.1097/HP.0000000000000116

The thickness of the combined salt layers at the WIPP repository is around 914 m and largely devoid of radionuclides other than that from ^{40}K (there are commercial potash mines in regional counties). The phenomenal amount of salt in this formation is insurance that there are no geological water transport mechanisms that could move the disposed transuranic (TRU) activity back into the biosphere. The salt at these depths is macroscopically plastic in nature, as it will slowly flow in such a way as to cocoon the waste over time due to the massive lithostatic pressures present at these depths.

The underground portion of the salt mine is regulated by the Mine Safety Health Administration and has to meet all the requirements associated with ventilation and airflow. These requirements include the proscriptive minimum ventilation rates for simple occupation up to that for large-scale operation of diesel equipment. Meeting these ventilation requirements is accomplished by placing large fans on the surface, which pull the unfiltered air through the mine and exhaust it on the surface. Neither the air being pulled from the surface nor the air exhaust is generally forced through filters. The unfiltered air pulled down through the air intake shaft is split up throughout the underground to provide the required ventilation for workers and operations. The air pulled into the mine contains suspended dirt, dust, and sand, which often occur when surface conditions are windy (with occasional dust storms). The land is semi-arid and generally contains >90% sand content in area soil with desert grass and shrubs sparsely distributed throughout the region. Similarly, dunes form around the larger shrubs are approximately 1 m in height. This soil contains all anthropogenic radioactivity present in the environment from nuclear weapons-related activities. This is somewhat problematic in that the waste being disposed of in the WIPP underground also contains some similar radioactivity due to nuclear weapons production activities. Long-term buildup of environmental anthropogenic activity in the underground and subsequent resuspension in the mine for release back to the environment therefore poses some challenges when discrimination of any radioactivity from WIPP operations is desired.

The exhaust air can be filtered just prior to release on the surface if there are radiological conditions, which could indicate that nuclear release from the waste is occurring. The effluent is monitored by fixed air samplers to demonstrate compliance with the U.S. Environmental Protection Agency (EPA) National Emission Standards for Hazardous Air Pollutants (NESHAPS) regulations (USEPA 2012) of no more than 10 mrem to an offsite individual from annual releases. These air samplers are situated in the exhaust flow and allow radiochemistry assay of all target isotopes of interest. It was use of these air samplers that first identified the presence of ^7Be in the WIPP effluent (CEMRC 2000; ^7Be is produced in the stratosphere by cosmic ray proton bombardment of carbon). This in turn indicated that surface radioactivity not related to radon progeny is pulled all the way through the mine and exits the exhaust.

Both radiochemistry and gamma spectrometry results are provided in this paper that support the hypothesis that mixing of anthropogenic surface TRU activity not related to WIPP operations is being pulled into the repository due to surface wind resuspension and related effects. The details of the experimental procedures used for assay of the salt scale and air filters are also provided.

BACKGROUND

Atmospheric weapons testing

Both ^{137}Cs and $^{238,239}\text{Pu}$ are ubiquitous in the environment due to atmospheric testing of nuclear weapons. Understanding their specific activity distributions spatially, and more importantly the ratio of their activity, can be used to fingerprint their source.

Weapons testing in the atmosphere was largely concentrated between the years 1952 to 1962 with a total fission and fusion yield of 545 Mt, having a total activity released to the atmosphere of 0.604, 0.912, 0.00652, 0.00435, and 0.141 EBq (10^{18} Bq) for ^{90}Sr , ^{137}Cs , ^{239}Pu , ^{240}Pu , and ^{241}Pu , respectively (UNSCEAR 1993). When considering only the 40-50 degree latitude for fallout, the National Institutes of Health (NIH) reported the values reproduced in Table 1 for both global and Nevada Test Site (NTS, now called NNSS) generated fallout density (NCI 2005). When specifically focusing on southeast

New Mexico, the ^{137}Cs deposition density was reported to be in the range of 1,000 to 3,000 Bq m^{-2} from global fallout but only 100 to 300 Bq m^{-2} for NTS fallout (Beck and Bennett 2002).

The actual bounding counties around the WIPP site, Eddy and Lea counties, were estimated specifically to have 1,500 to 3,000 Bq m^{-2} in ^{137}Cs by Beck and Bennett (2002). Using these with the Pu values from Table 1 would result in a Cs/Pu ratio ranging from 25 to 50.

The Trinity test in White Sands, NM, was an above-ground nuclear test (in fact the original) that took place on 16 July 1945. The fallout from this test would have had to travel southeast to reach the WIPP site, but the majority of it was measured to be deposited in a northeast direction (Fritzsche 1994), largely not affecting anthropogenic surface deposition near or around the WIPP site.

Project Plowshare

The Gnome site was part of the Project Plowshare program where the U.S. was trying to find peaceful applications for nuclear weapons, such as civil mining and excavating. The Gnome site was located only 5.5 miles from the current WIPP site boundary and was intended to demonstrate the capability to create underground caverns for storage of natural gas. When the detonation took place in 1961, the event created an unexpected venting of gases to the environment. The release created a plume footprint traveling north-northwest not too far from the present WIPP site location (Placak 1961). Because of this, the contribution from ^{90}Sr , ^{137}Cs , Pu, and Am from the Gnome release (Boyns 1973; Kenney et al. 1995) are all of concern for discriminating any environmental releases due strictly to WIPP operations.

Resuspension in the vicinity of the WIPP site

The variable dependencies for resuspension in New Mexico have been evaluated (Whicker et al. 2006) and found to have reasonable predictability, provided that enough meteorological and environmental parameters are known in terms of quantitative horizontal material transport (Breshears et al. 2012). Although the physics of resuspension in terms of particle size, velocity, and other parameters are approximate at best for environmental conditions (Ziskind et al. 1995), the actual resuspension threshold for the semi-arid conditions around the WIPP was measured by Arimoto et al. (2002) to start around 4 m s^{-1} wind velocity and then to plateau around 7 m s^{-1} . In other words, plutonium containing aerosols starts to increase in environmental air samples with winds of 4 m s^{-1} with a maximum at wind speeds of 7 m s^{-1} and staying constant at wind speeds above 7 m s^{-1} . Nonlinear responses above 7 m s^{-1} have been measured for episodic wind bursts, with 1 min measurements having an apparent threshold of 7 m s^{-1} with a concentration decreasing

Table 1. Select radionuclide fallout values for the contiguous United States reported for 2004 (Beck and Bennett 2002).

Nuclides	NTS	Global fallout in the U.S.
^{137}Cs	0.26 kBq m^{-2}	5.2 kBq m^{-2}
^{90}Sr	0.11 kBq m^{-2}	3.2 kBq m^{-2}
$^{239,240}\text{Pu}$	$\sim 0.015 \text{ kBq m}^{-2}$	0.06 kBq m^{-2}
$^{137}\text{Cs} / ^{90}\text{Sr}$	2.4	1.6
$^{90}\text{Sr} / ^{239,240}\text{Pu}$	7	53
$^{137}\text{Cs} / ^{239,240}\text{Pu}$	18	73

exponentially with height (Whicker et al. 2002). The region around the WIPP site has just under a 2% annual frequency of “dusty” hours from wind getting as high as 5% in March (Orgill and Schmel 1976) (with 3% being the highest yearly national average near Lubbock, TX), indicating a relatively expected high aeolian transport for the area.

As resuspended particulate in the surface air is pulled unfiltered into the WIPP mine, entrained with it are the ubiquitous anthropogenic radionuclides, including fission products and transuranics. Although the majority of the air comes in through the air intake shaft, smaller amounts come in through the salt and waste shafts. In normal mode, an approximate splitting would be 285 kcfm, 90 kcfm, and 50 kcfm through the air intake, salt, and waste shafts, respectively.

Previous work

There have been others who have considered the use of isotopic ratios to discriminate any releases from WIPP operations from the environmental anthropogenic activity ubiquitous to the area (Kirchner et al. 2002). As a continuation of that work, more current measurement information is available to be folded into a set of action levels and recommended future work to support quality environmental assessment determinations with specific attention toward the mine effluent.

Aeolian material deposition and transport in the mine

There are three identified material accumulation mechanisms on the air intake and salt shaft walls. The shaft is lined down to the start of the salt layer (approximately 274 m). The concrete lining cuts through the water table near the surface. Over the years, water has leaked down along the outer circumference of the lining and started to emerge into the air (due to turbulence) at the bottom of the lining. This is because the lining intersects the water table, and what small amounts have leaked down the lining can be picked up by the upward turbulent high velocity air and carried along with the effluent if it does not plate out lower down the shaft. Although this is a very small amount of water spray, it does contribute to surface deposition lower down in the shaft if it takes any dissolved salt with it, causing mixing, and some plates out on the shaft further down. Another mechanism for material growth on the shaft lining is brine leakage out of the salt itself. The salt layer does have ancient brine inclusions, which slowly migrate to the shaft over time and leave behind what looks like a small cauliflower branch when the brine dries subsequently. These protrusions also accumulate dust deposition from the adjacent air transport. The third material growth mechanism on the shaft interior is that basic dust and sand plate out from the entrained soil brought down with the intake air. All three

of these mechanisms can combine and were sampled by scraping for radiochemistry evaluation, which is described later in this paper. This material buildup has to be scraped off manually to prevent dangerous buildup. The criteria are somewhat subjective for when and how much to scrape or not, but the decision is given to an experienced certified miner to maintain minimal buildup on the shaft walls.

In addition, soil deposition at the base of the air intake shaft from Aeolian particulate has literally covered all exposed areas of the mine directly adjacent to the air intake shaft, with sand and dirt coloring it the same tan hue found on the surface as shown in Fig. 1a (typically the mined salt is white to light grey in color). This loess material slowly fades back to the original whites of the salt as one goes deeper into the mine due to dilution attributed to plate-out, as seen in Fig. 1b. The mine is, however, a fully functional and operational deep underground salt mine in every sense of the word, resulting in regular motion of diesel powered heavy machinery and ground control (which includes mining, hauling, drilling, bolting, and scraping salt), allowing regular forced resuspension of deposited material anywhere in the mine potentially at any given time (Fig. 2). These factors drive an expectation that environmental anthropogenic radionuclides would be more concentrated near the air intake shaft but present

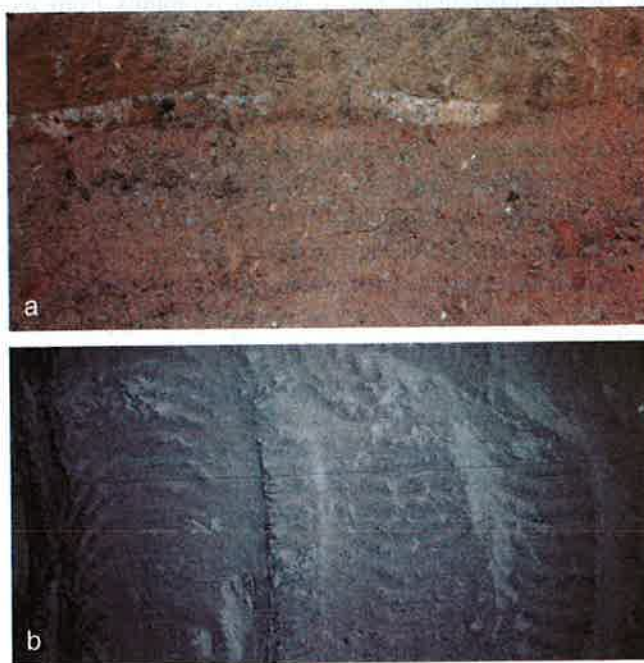


Fig. 1a. (top) Photo of the ground next to the mine rib (wall) in the WIPP underground taken at the base of the Air Intake Shaft (AIS). This photo shows the sand and dirt (mixed with and layered on top of salt) deposition due to natural plate-out. Figure 1b. Salt deposition on the ribs of the mine due to normal mine operations including ventilation and operation of various diesel equipment. The darker grey colors are due to diesel exhaust plate-out on the surface mixing and plating out with the salt dust.



Fig. 2. Salt samples taken from the base of the air intake shaft generated by biannual scraping of the salt shaft along its length to limit material buildup. The salt is in a poly sample bag, and the scale is approximately 1.5 in in height.

throughout the underground. In addition, it should be expected that portions of these radionuclides will be transported continually all the way through the mine to the air exhaust shaft and eventually out of the mine altogether.

Examples of the mine interior at the base of the AIS is shown in Fig. 1a, where the surface of the mine is largely covered in sandy dirt of identical color to that aboveground. This image can be compared to Fig. 1b taken much deeper into the mine, which shows the common color of the salt (mixed with some diesel emission plate-out) at various locations further from the AIS. Although the dominant colors change, there are no controls preventing or hindering in any way the transport of surface ground dirt from the AIS further into the mine due to normal operations. Fig. 2 shows scrapings from the base of the AIS used for radiochemistry.

Isotopic ratios

A standard historical method for discriminating source term radioactivity has been evaluation of isotopic ratios (Becker 2003). This can be done for a variety of applications, including nonproliferation verification (Glaser and Bürger 2009), nuclear forensics (Stanley et al. 2012), material characterization (Tandon et al. 2008), quality assay (Kutschera 2005), and a number of other applications (Meier-Augenstein 1999).

The environmental anthropogenic radionuclides in the vicinity of the WIPP have been studied rather extensively, characterized and quantified during the years prior to WIPP operations (Arimoto et al. 2005; Minnema and Brewer 1983) with offsite aerosol concentrations presented in Table 2 taken by the Environmental Evaluation Group (Gray and Ballard 2001) (a previous independent oversight organization). These can be compared to the aerosol measurements taken by WIPP and analyzed by various external subcontractors in the preoperational phase (USDOE 1999), which are presented in Table 3. In both cases, the uncertainties were quite large, and although an analysis of the probability distribution functions will not be carried out here, it is planned for subsequent analytical efforts.

Given the distribution of the values in Table 2, the isotopic ratios from this data are presented in Table 4.

Table 2. EEG preoperational baseline aerosol concentrations averaged over 1993 to 1999 prior to initiation of TRU waste receipt at WIPP (Gray and Ballard 2001).

Radionuclide	Effluent air			Ambient air		
	nBq m ⁻³	2 σ	N	nBq m ⁻³	2 σ	N
²⁴¹ Am	25	177	18	27	109	79
^{239,240} Pu	25	200	20	23	56	88
²³⁸ Pu	13	96	18	6	62	90
¹³⁷ Cs	880	7,800	23	60	2,460	104
⁹⁰ Sr	820	5,750	16	1,260	2,290	44

Another independent oversight group for the WIPP is the Carlsbad Environmental Monitoring and Research Center (CEMRC), which is part of the New Mexico State University complex. Preoperational environmental soil sample assay results taken by CEMRC from the WIPP vicinity are presented in Table 5.

CEMRC has also evaluated the ¹³⁷Cs/^{239,240}Pu ratios for soil samples both at the Gnome site and in the vicinity of the WIPP site, obtaining values of $(3.6 \pm 1.6) \times 10^3$ and 29.3 ± 0.4 , respectively (CEMRC 2007), which are clearly lower than the larger regional value for the ratio of 73 given in Table 1. Fixed Air Sampler (FAS) samples from both offsite and onsite that incorporate unfiltered outside air would also be subject to these criteria for isotopic ratios due to the expected environmental source terms.

The surface soil results from WIPP samples are presented in Table 6 from the preoperational results (USDOE 1999) as a comparison to the CEMRC results in Table 5, which demonstrate reasonable agreement.

MATERIALS AND METHODS

WIPP Labs Radiochemistry for fixed air samples[†]

The samples are traced with ²⁴²Pu, ²³²U, ²⁴³Am, and ²²Na. The ²²Na serves as a tracer for all gamma-emitting isotopes of interest. There is also a stable Sr carrier added for ⁹⁰Sr recovery determination. In general, air filter samples that are analyzed at WIPP Labs are split into two equal fractions after an acid digestion. For this reason, the normal amount of tracer is doubled. The samples and corresponding QC are digested in Teflon beakers with a combination of hydrofluoric acid (HF) and nitric acid (HNO₃). This is followed by the addition of boric acid to buffer the HF. The boric acid step is followed by an aqua regia digestion [1 part HNO₃, 3 parts hydrochloric acid (HCl)]. The samples are transferred to volumetric flasks after the digestion is complete and are split using Class A volumetric pipettes. One half of the sample is brought to 500 mL in a Marinelli beaker for gamma

[†]Current procedures for air filter assay are presented here; historical use of subcontractors is not addressed.

Table 3. WIPP off-site aerosol measurement prior to operational receipt of any TRU waste at the WIPP site (USDOE 1999). All assay units are in nBq m⁻³. The reported means in this table are the weighted averages.

Year	²⁴¹ Am		^{239,240} Pu		²³⁸ Pu		¹³⁷ Cs		Cs/Pu
	Mean	2 σ	Mean	2 σ	Mean	2 σ	Mean	2 σ	
1994	1,766	3 × 10 ⁴	-32	8 × 10 ⁴	60	4 × 10 ²	-587	1 × 10 ⁴	19
1995	2,979	1 × 10 ⁵	571	7 × 10 ³	-82	5 × 10 ³	3,144	2 × 10 ⁴	6
1996	199	2 × 10 ³	87	6 × 10 ²	45	9 × 10 ⁵	2,272	1 × 10 ⁴	26
1997	-27	8 × 10 ¹	4.6	2 × 10 ¹	-0.9	1 × 10 ²	5,456	1 × 10 ⁴	1,181
1998	231	3 × 10 ²	115	2 × 10 ²	-30	3 × 10 ²	18,043	6 × 10 ³	157
Average	1,030	3 × 10 ⁴	149	2 × 10 ⁴	-2	2 × 10 ⁵	5,665	1 × 10 ⁴	278

analysis. The other half is transferred to a glass beaker and taken to dryness, and separation of the various alpha emitting isotopes as well as beta-emitting ⁹⁰Sr is completed.

The residue is dissolved in 7 mL of 6 M HNO₃, and after the sample is in solution, 7 mL of 2 M Al(NO₃)₃ is added. The oxidation states of the analytes of interest are adjusted in preparation for column separation. The Pu must be adjusted to the +4 state, the U is adjusted to the +6 oxidation state, and the Am and Sr remain in their normal states of +3 and +2, respectively. The oxidation state adjustments are performed as follows: 0.5 mL of 1.5 M sulfamic acid and 1.25 mL of 1.5 M ascorbic acid are added to the solution. The solution is mixed well and allowed to stand for 3 min. Finally, 2 mL of 3.5 M sodium nitrite is added to the solution to oxidize the Pu to +4.

TEVA, TRU, and SR resin cartridges (Eichrom, Lyle, IN, USA) are stacked to perform the radiochemical separations. The Pu binds to the TEVA resin, and Am and U pass through the TEVA resin and bind to the TRU resin. The Sr passes through the TEVA and TRU resins and binds to the SR resin. After the initial load solution passes through, the columns are separated. The TEVA resin is rinsed with 8 M HNO₃ followed by 3 M HNO₃. Thorium is eluted from the TEVA resin using 9 M HCl. A final rinse with 3 M HNO₃ is done before eluting the Pu with an 0.1 M/0.05 M/0.03 M HCl/HF/Titanium(III)Chloride solution. The TRU resin is rinsed with 2 M HNO₃ followed by 0.5 M HNO₃. Am is eluted from the TRU resin using 4 M HCl. A rinse with a solution of 4 M/0.2 M HCl/HF and a final rinse with 4 M HCl are done before eluting the U with 0.1 M ammonium bioxalate. The alpha emitters are microprecipitated with NdF₃ and mounted onto Eichrom

Table 4. Isotopic ratios for the preoperational baseline data from Table 1.

	Effluent air	Ambient air
¹³⁷ Cs/ ^{239,240} Pu	35 ± 420	3 ± 107
¹³⁷ Cs/ ⁹⁰ Sr	1 ± 12	0.05 ± 2
⁹⁰ Sr/ ^{239,240} Pu	33 ± 349	55 ± 166
^{239,240} Pu/ ²⁴¹ Am	1 ± 11	1 ± 4
^{239,240} Pu/ ²³⁸ Pu	2 ± 21	4 ± 41

Resolve Filters (0.1 micron porosity) for analysis by alpha spectroscopy. The SR resin is rinsed with 8 M HNO₃. After this rinse has been completed, time is recorded as the yttrium ingrowth time. Sr is eluted from the column with 0.05 M HNO₃. The Sr is precipitated out as SrCO₃, and the recovery is determined gravimetrically before analyzing ⁹⁰Sr by gross proportional counting.

WIPP Labs Radiochemistry for AIS salt samples[†]

Upon arrival in the lab, the samples are weighed and placed in a drying oven at 110°C. After drying, the samples are tumbled in a jar mill overnight to homogenize them. A 2-g portion of the sample is taken for Pu and Am analyses. The samples are traced with ²⁴²Pu and ²⁴³Am. The samples and corresponding QC are digested in Teflon beakers with a combination of hydrofluoric acid (HF) and nitric acid (HNO₃). This is followed by the addition of boric acid to take care of the HF. The boric acid step is followed by an aqua regia digestion (1 part HNO₃, 3 parts hydrochloric acid HCl). The samples are transferred to glass beakers and are taken to dryness.

The residue is dissolved in 7 mL of 6 M HNO₃, and after the sample is in solution, 7 mL of 2 M Al(NO₃)₃ is added. The oxidation states of the analytes of interest are adjusted in preparation for column separation. The Pu must be adjusted to the +4 state, and the Am remains at the +3 oxidation state as normal. To adjust the Pu to +4, 0.5 mL of 1.5 M sulfamic acid and 1.25 mL of 1.5 M ascorbic acid are added to the solution. The solution is mixed well and allowed to stand for 3 min. Finally, 2 mL of 3.5 M sodium nitrite is added to the solution to oxidize the Pu to +4. Eichrom TEVA and TRU resin cartridges are stacked to perform the radiochemical separations. The Pu binds to the TEVA resin while the Am passes through the TEVA resin and binds on the TRU resin. After the initial load solution passes through, the columns are separated. The TEVA resin is rinsed with 8 M HNO₃ followed by 3 M HNO₃. Thorium is eluted from the TEVA resin using 9 M HCl. A final rinse with 3 M HNO₃ is done before eluting the Pu with 0.1 M/0.05 M/0.03 M HCl/HF/Titanium(III)Chloride. The TRU resin is rinsed with 2 M HNO₃ followed by 0.5 M HNO₃. Am

Table 5. CEMRC soil measurements in the WIPP vicinity prior to TRU waste receipt (CEMRC 2000).

Radionuclide	Cactus flats			Near field			1997 Report (CEMRC 1998)		
	mBq g ⁻¹	2 σ	N	mBq g ⁻¹	2 σ	N	mBq g ⁻¹	2 σ	N
²⁴¹ Am	0.083	0.007	40	0.049	0.004	31	0.066	0.0010	9
^{239,240} Pu	0.22	0.02	48	0.10	0.007	48	0.14	0.002	16
²³⁸ Pu	0.022	0.003	7	0.045	0.017	4	—	—	—
¹³⁷ Cs	6.2	0.5	48	3.1	0.2	48	4.5	6.9	48
²³⁸ U	8.9	0.3	48	7.7	0.2	48	4.2	0.3	16

is eluted from the TRU resin using 4 M HCl. The samples are microprecipitated with NdF₃ and mounted onto Eichrom Resolve Filters (0.1 micron porosity) for analysis by alpha spectroscopy.

The remaining solid portion of the sample was used for gamma analysis. To match one of the standard geometries used by the lab, the solid sample was mixed into a slurry with water to 3 cm from the bottom of a 125-mL jar.

Gamma spectrometry in the WIPP underground

The gamma spectrometry was carried out using an ORTEC Micro-HX portable high purity germanium spectrometer (ORTEC, Atlanta, GA, USA). The physical configuration was to put the spectrometer against one wall with the detector pointed out toward the open drift perpendicular to the axis of the crystal. Multiple spectra were taken starting at the bottom of the shaft and extending deep into the mine using spectral accumulation times of at least 1 d but less than 1 wk per spectrum. All measurements were taken from April to June 2011.

The Monte Carlo modeling to convert the spectral data into assay estimates was carried out using the MCNP5 software (X-5 Monte Carlo Team 2003) version 5.1.2600 on an HP xw9400 workstation. An example of the input stacks used to simulate this configuration is given in Appendix A.

Expected probability distribution from the ratio of standard normal deviates

In order to carry out a statistical comparison of isotopic ratios as proposed in this work, the statistics of ratios of this kind must be considered. If either the numerator

or denominator were consistently much larger than unity, the ratio could be approximated readily by more familiar distributions, but when the ratio approaches the ratio of two null values with either of them possibly being negative, some interesting results can be realized. The current work involves analyzing isotopic ratios of anthropogenic radionuclides at environmental levels, with the act of subtracting background results in isotopic ratios having the possibility of one or both the numerator and denominator being very close to zero and even negative (due to background subtraction). The relevant derivations from this effect are relegated to Appendix 2, although the fundamentals of the Cauchy distribution [with the Cauchy density being of the form $f(x) = a/(1 + x^2)$] have been discussed in much more detail elsewhere (Knight 1976; Huang and Chen 2007; Doric 2011); the reader is directed there for more rigorous mathematical analysis.

There are two pertinent generalizations of the resulting distribution (for the ratio of two random variables) that are both demonstrated and relevant to the current work. One is that when the uncertainties are large compared to their respective variables, the probability density function will have a Lorentzian-like distribution. The second is that when the mean of the ratio is large compared to unity with the numerator having uncertainty comparable to the variable (allowing it to become negative), the resulting distribution will be multimodal. The latter effect is caused by a typically small probability of having the ratio fall arbitrarily close to zero (when the numerator becomes zero) with larger absolute values more likely near the true mean. This latter effect is realized

Table 6. WIPP subcontracted assay of soil measurements in the WIPP vicinity prior to TRU waste receipt (CEMRC 2000). Here TPU is the total propagated uncertainty at the 1 standard deviation level.

Location	²⁴¹ Am		^{239,240} Pu		²³⁸ Pu		¹³⁷ Cs		⁹⁰ Sr	
	mBq g ⁻¹	TPU	mBq g ⁻¹	TPU	mBq g ⁻¹	TPU	mBq g ⁻¹	TPU	mBq g ⁻¹	TPU
SE Contr.	0.22	0.52	0.74	0.41	0.19	0.30	7.8	4.8	-292	70
WIPP East	0.11	0.41	0.15	0.22	0.26	0.41	8.5	3.4	12	18
WIPP South	1.04	1.11	0.15	0.26	-0.11	0.48	4.8	3.7	8	18
Mills Ranch	0.00	0.52	0.67	0.81	-0.15	0.48	15.9	4.8	37	21
WIPP FF	-0.11	0.41	0.52	0.56	0.41	0.52	0.9	3.3	-7	12
Smith Ranch	0.07	0.44	0.52	0.59	0.00	0.81	-0.6	3.7	30	21
Weighted average	0.08	0.20	0.28	0.14	0.13	0.18	5.2	1.6	5.8	7.4

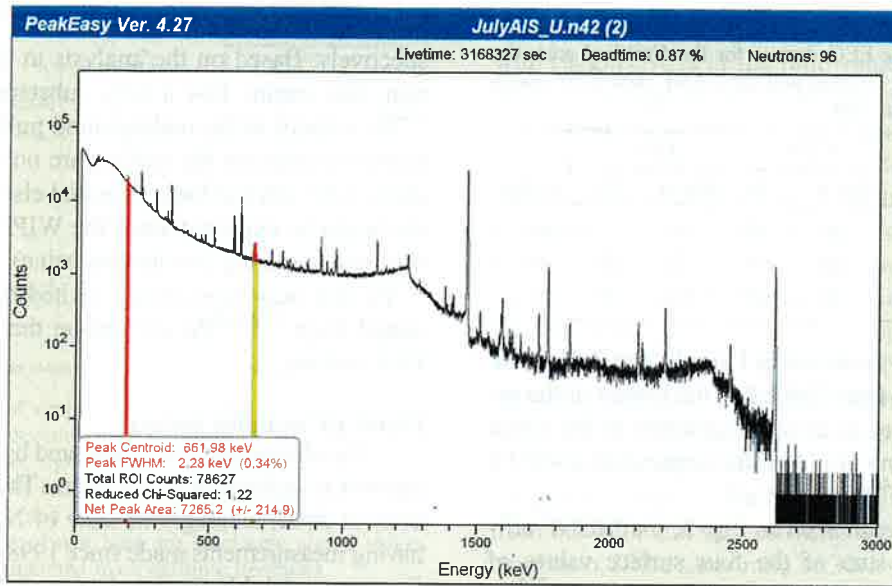


Fig. 3. Long acquisition HPGe spectrum in the WIPP underground near the Air Intake Shaft (AIS) showing both the ^{226}Ra and ^{137}Cs (at 186 keV and 662 keV, respectively) peaks highlighted along with ^{40}K and various radon progeny peaks (not highlighted). The curve fit statistics for the ^{137}Cs peak are shown in the bottom left of the figure.

when the mean ratio is large and the numerator approaches zero; the denominator must also be near zero not to result in an almost zero ratio (hence creating a minimum near zero in the distribution). The large tails in the Lorentzian distribution result when the denominator gets close to zero with the numerator taking any nominal value. Similarly, if the ratio is large due to a substantially greater numerator than denominator and the uncertainty is small enough in both values to prevent it from obtaining negative values, the distribution can be approximated with a Gaussian (Liu et al. 2012) form (although this latter effect will not be demonstrated here, as it is not used). In general, however, numerical integration is currently required for all non-symmetric intervals and for all intervals of non-symmetric distributions (where the mean of the ratio is not unity with large uncertainty).

RESULTS AND ANALYSIS

Underground in situ gamma spectrometry assay

An example of a long accumulation gamma spectrum obtained in the WIPP underground near the AIS is shown in Fig. 3. This particular spectrum was the result of almost 7 d of integrated counting. The spectrum shows both a ^{226}Ra and a ^{137}Cs peak due to dust plating out all over the drifts near the AIS. These peaks are expected results given the large surface soil deposition occurring in the underground (see Fig. 1a). Using the expected ratio of $^{137}\text{Cs}/^{239,240}\text{Pu}$ for ambient air given in Tables 1 or 4 allows a quantitative estimation of the $^{239,240}\text{Pu}$ content in the underground without having to carry out extensive mass spectrometry measurements.

The general features shown in Fig. 3 were identified at around 150 m down-flow in the drift where the air was turbulent after turning horizontal from the vertical air intake shaft. The count rate of the ^{226}Ra peak and the ^{137}Cs peaks in Fig. 3 were found to be 9.4×10^{-3} and 2.3×10^{-3} counts s^{-1} , respectively.

The results of the *f8 efficiency calculation[†] done below using the MCNP model (see Appendix 1) resulted in the four surfaces for each portion of the mine access corridor coming off the AIS having a calculated contribution to the ^{137}Cs peak of 3.31, 0.69, 2.51, and 0.45 in units of 10^{-7} MeV per starting photon for the floor, back, adjacent wall, and far wall, respectively (totaling 6.96×10^{-7} MeV per source particle). Converting this into an activity per area is done in eqn (1), where the isotope branching ratio, energy normalization, total surface area (of 2.43×10^7 cm^2), and unit conversions are all carried out:

$$\frac{2.3 \times 10^{-3} \frac{\text{counts}}{\text{s}} \times 0.662 \frac{\text{MeV}}{\text{count}}}{24.3 \times 10^6 \text{ cm}^2 \times 0.8998 \frac{\text{starting particle}}{\text{disintegrations}} \times 6.96 \times 10^{-7} \frac{\text{MeV}}{\text{starting particle}}} = 1 \times 10^{-4} \frac{\text{Bq}}{\text{cm}^2} \quad (1)$$

Assuming all mine surfaces are uniformly deposited with the surface particulate, the resulting estimate of the total ^{137}Cs activity in that section of the drift alone becomes 2.4×10^3 Bq. Using a ratio value of 3 from Table 4 would put the $^{239,240}\text{Pu}$ assay estimate from this at approximately 8.1×10^2 Bq, whereas the ratio value of 73 from Table 1 would give a $^{239,240}\text{Pu}$ activity of only 33 Bq.

Clearly this activity would not all be delivered to the effluent, but it does represent a current TRU content in the

[†]All *f8 tallies passed the internal MCNP statistical checks with an average relative error at the 0.662 MeV bin of around 1%.

Table 7. Average actinide air concentrations for New Mexico (Kenney et al. 1998). The EEG data is for the Carlsbad area, the EPA data is for the Santa Fe area, and the LANL data is for Santa Fe, Espanola and Pojoaque NM.

Isotope	EEG		LANL		EPA		average
	nBq m ⁻³	2σ	nBq m ⁻³	2σ	nBq m ⁻³	2σ	
²⁴¹ Am	29	48	130	93	—	—	80
^{239,240} Pu	30	28	110	280	7	22	49
²³⁸ Pu	14	35	70	100	11	15	32

underground surfaces as shown in Figs. 1a and 2. The use of $^{137}\text{Cs}/^{239,240}\text{Pu} = 3$ from Table 2 is the lowest of the ratio values and so serves as an approximation to the upper bound of $^{239,240}\text{Pu}$ content in that the expression could be rewritten to read $^{239,240}\text{Pu} \leq ^{137}\text{Cs}/3$.

With the ^{226}Ra result seen in Fig. 3, the MCNP efficiency result gave a sum of the four surface values of 6.56×10^{-7} MeV per starting particle resulting in a ^{226}Ra assay estimate of 74 kBq as shown in eqn (2). Using an assumed equilibrium activity ratio of $^{238}\text{U}/^{226}\text{Ra} = 0.8$ [based on the NCRP average content for soil (NCRP 1988), although values as high as unity (Patra et al. 2012) or even less than a half (Hamilton 1989) are also in the literature] gives the resulting activity estimates of ^{238}U as 59 kBq:

$$\frac{9.4 \times 10^{-3} \frac{\text{counts}}{\text{s}} \times 0.186 \frac{\text{MeV}}{\text{count}} \times 1 \text{Bq}/(\text{disintegrations/s})}{0.0359 \frac{\text{starting particle}}{\text{disintegrations}} \times 6.56 \times 10^{-7} \frac{\text{MeV}}{\text{starting particle}}} = 74 \text{ kBq}. \quad (2)$$

Air transport intake estimate

Another method to estimate total environmental $^{239,240}\text{Pu}$ content in the underground would be to use the aeolian transport mechanism to calculate how much resuspended material would have been in the WIPP intake air. At the WIPP, the mine intake airflow is monitored throughout the year (WTS 2011a), and so the annual volume taken in can be approximated by the product of the average flow rate and the time, resulting in an average volume of $1.8 \times 10^{11} \text{ m}^3$. Using the average surface actinide concentrations in air from Table 7, the total estimated average activity pulled into the WIPP mine since 1983 [the year when the first underground storage room and the exhaust shaft had been mined out fully and completed (Rechard 1999)] would then be approximately 14 kBq,

8.5 kBq, and 5.5 kBq for ^{241}Am , $^{239,240}\text{Pu}$, and ^{238}Pu , respectively. Based on the analysis in the previous subsection, this means that a very substantial majority of the ^{239}Pu activity in the underground pulled in from environmental sources on the surface are no longer in the access drift to the AIS but have migrated elsewhere into the mine (as might be expected since the WIPP is a fully functioning and operating production mine). How much of this ^{239}Pu that may have already exited the mine can be estimated from $^{239,240}\text{Pu}$ content on the effluent monitoring FAS stations.

Fixed air sampler assays

The effluent has been measured by three different radiochemistry facilities in recent years. The EEG ceased operations in 2002, although the state of New Mexico has been having measurements made since 1998 through the Carlsbad Environmental Monitoring Center (CEMRC), which is a part of the New Mexico State University complex. Table 8 contains all the data obtained since WIPP began operations from all three groups (including those from the management and operating contractor of the WIPP site).

Other values from the $^{137}\text{Cs}/^{239,240}\text{Pu}$ ratio can be obtained from Tables 5 and 6. The ratios found there range from -1.2 up to 57 . A weighted average using standard quadrature error propagation (to calculate the weights) gives a result of 24 from these values.

Statistical comparison of ratio measurements

The large uncertainties seen in Table 4 reflect the inherent difficulties associated with measuring values that are similar to background. Further attempting to evaluate ratios of such numbers becomes even more problematic when values can be both negative and very close to zero. The brief review given in Appendix B demonstrates that without making some gross assumptions, the confidence limits from the ratio can be both highly skewed and include negative values. As shown in Appendix B, integration is required to obtain functionally quantitative confidence limits for this kind of distribution, as it is dependent upon both the mean of the numerator and the denominator (assuming both come from the fixed population distributions). This was carried out using a Monte Carlo (MC) spreadsheet

Table 8. Air sample assay values post operations at WIPP.

Measurement institution	²⁴¹ Am nBq m ⁻³	^{239,240} Pu nBq m ⁻³	²³⁸ Pu nBq m ⁻³	¹³⁷ Cs nBq m ⁻³
EEG off site	12 ± 41	12 ± 12	4 ± 16	936 ± 806
EEG effluent	59 ± 79	47 ± 42	34 ± 43	723 ± 2840
CEMRC off site (CEMRC 2010)	3.6 ± 1.9	10 ± 5	0.23 ± 0.66	97 ± 170
CEMRC effluent (CEMRC 2010)	25 ± 24	167 ± 52	7 ± 31	(-5 ± 18) × 10 ³
WIPP offsite [§]	17 ± 3	5 ± 3	0.9 ± 3	1647 ± 891

[§]Values obtained by th WIPP site's own environmental monitoring capability; all values are from weighted average calculation.

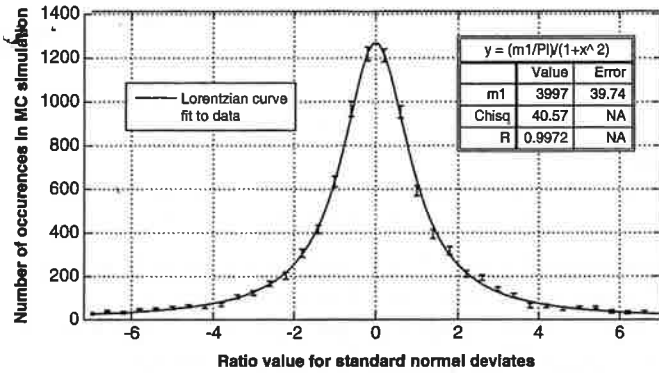


Fig. 4. Demonstration of simple functional form for the histogram distribution of normal deviate ratios. The functional form shown as the inset in the upper right of the figure was obtained using the Levenberg-Marquardt (non-linear least squares) fit from the Kaliedagraph© software and shows negligible deviation from the modeled functional form. Error bars are stochastic sigma values for each histogram bar obtained from multiple iterations.

technique (Hayes 2004) for generating random deviates. Taking the ratio of the deviates as described in Appendix 2 with $a = b = 0$, y and x being standard normal deviates followed by generating a histogram of the results is shown in Fig. 4.

As seen in Fig. 4, the functional form of the Lorentzian profile is unmistakable based on the curve fit and in this case has a unity full width at half maximum (FWHM) along with a zero offset. This result demonstrates agreement with the predicted functional form of a Lorentzian profile given in Appendix B with unity FWHM and zero bias. The error bars were single standard deviations of each bin empirically derived from 50 random MC generated distributions. The graph is actually a histogram, although the frequency bars are not shown to allow better resolution of the functional fit and the inherent variation in values represented by the error bars. The

distribution shown is generated from 1×10^4 occurrences, with roughly 90% of the ratio values shown in the figure having a histogram bin width of 0.4.

When the deviates do not have a symmetric distribution, the results from Appendix B demonstrate that higher moments can take place in the distribution. Carrying out the analysis using a ratio of 30 is shown in Fig. 5. From this kind of analysis, it can be approximated that when the numerator and denominator are biased by 30 and 1, respectively, the probability of an occurrence between 1 and 100 is only 76%, with an 86% chance of having a ratio fall between -100 and $+100$. Note that in this special case, only 16% of the distribution is negative.

The asymmetry seen in Fig. 5 is being driven by the combined effect of the denominator approaching zero from the right and then crossing the origin creating a negative ratio. If the same ratio of 30:1 were simulated having an uncertainty small compared to unity, a more symmetric distribution centered near 30 would be generated.

In general, whenever the denominator is close to the value of the inherent noise in the measurements, the bimodal distribution shown in Fig. 5 will be present to some extent. At much higher values, the distribution will not be symmetric but will have a single mode. Similarly, with measurements much higher than the inherent noise, the distributions can be roughly approximated by a Gaussian distribution, although technically a non-symmetric distribution will be present whenever the ratio mean is non-unity (e.g., $a/b \neq 1$; see Appendix B).

Plate out and release

The air intake shaft (AIS) liner has a minimum diameter of 5.1 m (with the salt section having a 22% larger initial diameter to allow for salt creep), and the salt shaft has a diameter of 3 m. Using eqn (3), the Reynolds

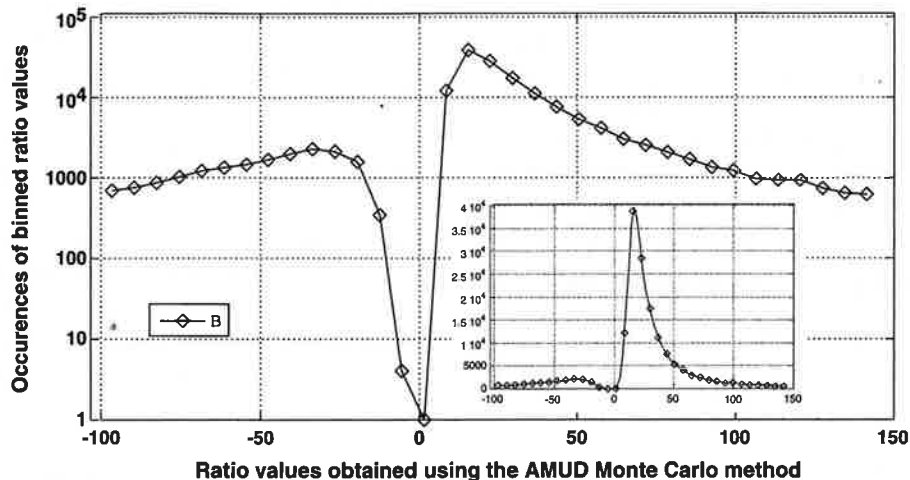


Fig. 5. Distribution from ratio values of 30:1 with normal deviates. The main graph is in semilog format with the inset having a linear abscissa scale. Note that the dominant mode is near 15 even though the true mean is 30.

Table 9. Salt sample ratio results from the current WIPP air intake shaft. Uncertainties are at the 95% CL and derived by quadrature from the individual assay results.

Isotopic ratio	s1	s2	s3	s4	s5	s6	s7	s8
$^{137}\text{Cs}/^{239,240}\text{Pu}$	-12 ± 22	-16 ± 197	-19 ± 65	18 ± 4	-4 ± 53	4 ± 39	-39 ± 194	123 ± 284
$^{239,240}\text{Pu}/^{241}\text{Am}$	0.6 ± 2	1 ± 32	-0.2 ± 1	2 ± 14	0.08 ± 0.3	1 ± 2	-0.3 ± 1	0.1 ± 0.3
$^{239,240}\text{Pu}/^{238}\text{Pu}$	0.4 ± 1	0.3 ± 2	0.4 ± 1	-16 ± 364	0.3 ± 1	0.8 ± 1	-2 ± 14	0.3 ± 0.5

number R can be calculated to be $>1 \times 10^6$ for the AIS (using the values of $\mu = 18.6 \times 10^{-6}$ Pa-s, $V = 4.7$ m s $^{-1}$, $d = 5.1$ m, $\rho = 1.225$ kg m $^{-2}$), which is well above the upper critical value of 4,000 for laminar flow (Vennard and Street 1975), indicating the flow is quite turbulent. As such, the turbulent airflow provides a mechanism such that the entrained particulate can be made to plate out on the shaft surfaces through impaction. This plate-out provides a sample of the source term (Fig. 2) known to be being pulled through the mine, which can be evaluated for isotopic ratio values:

$$R = V \times d \times \rho / \mu. \quad (3)$$

AIS salt samples

The radiochemistry results, in terms of the resulting isotopic ratios from the multiple salt samples, are presented in Table 9. The magnitude of the radiochemistry assay for the salt samples is considered somewhat arbitrary, as the salt content was not controlled for comparison since these were actual samples removed from the surface of the AIS caused by plate-out (as discussed above). Only the location of the air intake shaft is considered significant as this represents a definitive source term for the WIPP underground, which has no credible means of being contaminated from any of the WIPP operations. ** Examples of salt samples used to generate these values are shown in Fig. 2. The variety represents the mix of different source terms available for causing buildup on the shaft lining and walls.

All the values shown in Table 6 are consistent with background preoperational values from Tables 1 through 3 due to the large uncertainties, and they demonstrate the difficulty associated with evaluating measurement ratios from sample results near background levels. Multiple entries are seen to be negative and all overlap the origin as expected from the distribution described in Appendix B and shown in Fig. 5 as a special case.

Emplaced CH waste isotopic ratio distributions

Because the WIPP is only licensed for transuranic waste, the ratio of ^{137}Cs to $^{239,240}\text{Pu}$ tends to be extremely low for Contact Handled (CH) waste, and the proportion of currently emplaced waste having this ratio is very

small, as shown in Fig. 6 (using a log-log format). Here the data are presented in a histogram format, with the bins having no CH excluded from the figure. Only CH inventories are presented here because RH waste is only transported in heavy casks with no credible release mechanism (WTS 2011b; as CH could be breached by the tines of a fork truck or crushed in an accident). The occurrences of CH waste containers currently emplaced in the underground having $^{137}\text{Cs}/^{239,240}\text{Pu}$ ratios in the range of environmental values are indicated in Fig. 6 using the double arrow.

The total proportion of CH TRU waste containing both ^{137}Cs and $^{239,240}\text{Pu}$ and having a ratio in the range of 1 up to 100 is only 0.061%. So with less than 1/10th of 1% having a $^{137}\text{Cs}/^{239,240}\text{Pu}$ ratio in the range of environmental values, this is a rather strong test parameter for comparison when total magnitudes are also in the range of levels expected from environmental accumulation. Similarly, the percentage of containers having a reportable ^{137}Cs content was just over 21%, which then constitutes the only emplaced waste having any potential for a non-zero $^{137}\text{Cs}/^{239,240}\text{Pu}$ ratio in the environmental range. Note that this distribution would no longer be applicable if there were ever a breached RH container, although the relative percentage of waste having a $^{137}\text{Cs}/^{239,240}\text{Pu}$ ratio in the range of 1 to 100 when including RH is still only 1.3%.

Comparison of current measurements with historical values

The value calculated in eqn (1) results in a surface activity level of approximately 100 Bq m $^{-2}$, which is consistent with the range estimate of 0–1,000 Bq m $^{-2}$ for the area (Beck and Bennet 2002) for total ^{137}Cs deposition in the region.

The $^{137}\text{Cs}/^{239,240}\text{Pu}$ ratio of 29 reported by CEMRC (2006) seems to fall into the best agreement with general values calculated for the region by Beck and Bennet (2002). This is also true for the soil source term measurements from Tables 5 and 6 having an overall arithmetic mean of 23 ± 17 . A weighted average of the same group of numbers results in a ratio estimate of 24. The values from Table 5 alone are much more self-consistent, with an arithmetic mean of 30 ± 2 but from only three data points.

Typical ^{137}Cs concentrations for soil around the WIPP site prior to being operational were measured in 1982 to be approximately 4 mBq g $^{-1}$ (Minnema and

**Fresh air intake independent of exhaust air is required as a protective control in the event that an underground fire were to occur, to insure that there is fresh air to which miners can go to with their self rescuers and so safely escape the smoke.

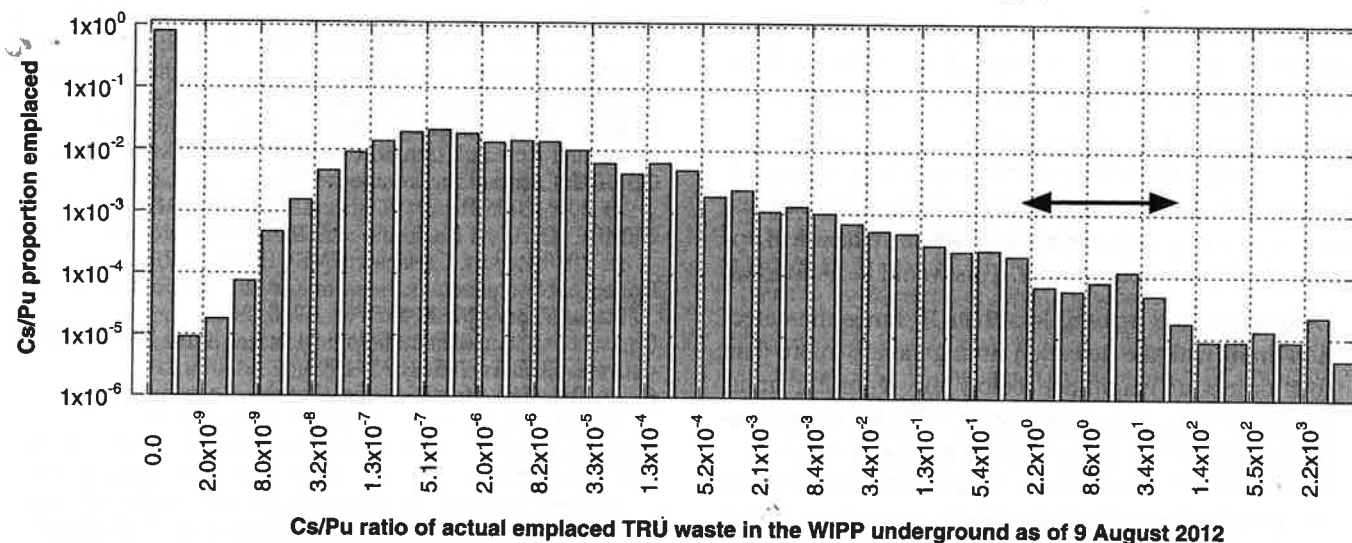


Fig. 6. Histogram of emplaced waste as a function of its Cs/Pu ratio with the range of environmental values shown by the double arrow. Those containers having no reported Cs were included in the zero bin at the left. Note this is a log-log distribution with over 200,000 occurrences binned with values normalized to give a probability distribution (unit area).

Brewer 1983), which would place the $^{239,240}\text{Pu}$ content around 1 mBq g^{-1} (using the $^{137}\text{Cs}/^{239,240}\text{Pu}$ ratio), demonstrating reasonable consistency with Table 6.

DISCUSSION AND CONCLUSION

Recommended ratio interpretations

In order for positive assays to require grading, this will in general require that the ^{137}Cs be larger than the $^{239,240}\text{Pu}$ content. The reason for this is that without long-term trending of positive and negative values of the ratio being instituted with retrospective statistical analysis, operational interpretation of negative ratio values is not useful. Although this could be part of a QA program or routine data analysis evaluation, being able to evaluate each current measurement based on historical measurements is generally not a standard practice for ratio values. With the additional potential for other bias to be present, careful consideration of acceptance limits needs to be applied.

Furthermore, the $^{239,240}\text{Pu}$ assay has release limits that are many orders of magnitude smaller than those for ^{137}Cs . When the $^{239,240}\text{Pu}$ assay results in a negative value after all background subtractions, the ^{137}Cs limits are generally not a concern. This is because ^{137}Cs effluent limits are many orders of magnitude higher than environmental levels, so measurements have been many orders of magnitude below reportable values. It is typically only the case that a detectable level of $^{239,240}\text{Pu}$ is of concern in determining whether the activity could have come from WIPP operations rather than the current ubiquitous background.

Further study of the details of these interpretations is certainly warranted and could prove to be a rich topic

for future research and development efforts with clearly a great deal of additional work to be done to understand these mechanics better. That said, allowing the ratio to range from 1 up to 100 appears to reasonably bound environmental measurements of background for the $^{137}\text{Cs}/^{239,240}\text{Pu}$ ratio.

Comparing the pre- and post-operational data, no statistically significant difference can be found, meaning no changes have been validated through measurements to date. This does not address the magnitude of the activity measured but does show that the activity appears to be of the same nature as the ubiquitous anthropogenic background.

Recommended future topics for research

What has not been addressed in this work is whether there is any basis to expect a change in the ratio values from what is taken into the mine from the environment until it eventually migrates out to the effluent. That is to ask whether there are any credible mechanical or even chemical changes present in the mine environment that transport through the drifts and might fractionate or influence the isotopic ratios. None are postulated at this moment, but this does not rule out the possibility that something like this could be occurring. Because the salt and diesel are not highly reactive, this is not considered an anticipated effect.

Only the use of previously established statistical models was used. As a result of this, uncertainties in individual assay values used in the ratios were not accounted for in any way other than the assumption that these uncertainties were adequately represented in the distribution of the assay values themselves. Use of the methods in Appendix B was qualitatively able to show that the

distributions are functionally consistent with the Cauchy distribution. The actual magnitude of any individual isotopes is a separate topic intended for a future paper.

Graded approach to action limits

Still, with a reasonable distribution of expected isotopic ratios for environmental anthropogenic radionuclides, some use of the measurements can be made in the use of operationally friendly action levels. This would be as follows:

- Detectable TRU activity less than 10 times the detection limit (with the detection limit generally more than four orders of magnitude below the reporting limit) having isotopic ratios consistent with the ubiquitous background are to be considered inconsequential;
- Detectable TRU greater than 10 but less than 1,000 times the detection limit should have backup samples checked and a notification made to the environmental monitoring and radiological control groups along with the ALARA coordinator for all assay results; and
- Detectable TRU greater than 1,000 times the detection limit should follow the previous bullet and be elevated further to the attention of the Nuclear Review Board (which consists of middle and senior management).

Guidance is not currently permitted in terms of making statistically significant determinations on actual activity magnitude, but this is planned for a future paper.

Author's note—The WIPP fire and radiological release of February 2014 have subsequently changed the paradigm at the WIPP site but not the science. The methods and results from this paper are useful for the current WIPP site and other locations requiring proper consideration of all temporal source term distributions in subsequent analyses.

Acknowledgments—This work paid for under U.S. DOE contract numbers DE-AC29-01AL66444 and DE-EM0001971.

REFERENCES

- Arimoto R, Kirchner T, Webb J, Conley M, Steward B, Schoep D, Walthall M. ^{239,240}Pu and inorganic substances in aerosols from the vicinity of a waste isolation pilot plant: the importance of resuspension. *Health Phys* 83:456–470; 2002.
- Arimoto R, Webb JL, Conley M. Radioactive contamination of atmospheric dust over southeastern New Mexico. *Atmospheric Env* 39:4745–4754; 2005.
- Beck HL, Bennett BG. Historical overview of atmospheric nuclear weapons testing and estimates of fallout in the continental United States. *Health Phys* 82:591–608; 2002.
- Becker JS. Mass spectrometry of long-lived radionuclides. *Spectrochimica Acta Part B* 58:1757–1784; 2003.
- Boyns PK. Radiological survey of the area surrounding the Project Gnome Test Site, Carlsbad, New Mexico, Date of Survey: 13 May 1972. Las Vegas, NM: Las Vegas Area Operations; EGG-1183-1569, EG&G ARMS Aerial Radiological Measuring System; 1973.
- Breshears DD, Kirchner TB, Whicker JJ, Field JP, Allen CD. Modeling aeolian transport in response to succession, disturbance and future climate: dynamic long-term risk assessment for contaminant redistribution. *Aeolian Res* 3:445–457; 2012.
- CEMRC. Carlsbad Environmental Monitoring and Research Center 1997 Report. Carlsbad, NM: CEMRC; 1998.
- CEMRC. Carlsbad Environmental Monitoring and Research Center 1999 Report. Carlsbad, NM: CEMRC; 2000.
- CEMRC. 2005/2006 Report Carlsbad Environmental Monitoring and Research Center. Carlsbad, NM: CEMRC; 2006.
- CEMRC. Carlsbad Environmental Monitoring & Research Center 2005/2006 Report. Carlsbad, NM: CEMRC; 2007.
- CEMRC. Carlsbad Environmental Monitoring & Research Center 2010 Report. Carlsbad, NM: CEMRC; 2010.
- Doric D. New generalizations of Cauchy distribution. *Comm Statist Theory Meth* 40:3764–3776; 2011.
- Fritzsche AE. An aerial radiological survey of the Trinity Fallout Area. *EGG* 1:1265–1037; 1994.
- Geary RC. The frequency distribution of the quotient of two normal variates. *J Royal Statist Soc* 93:442–446; 1930.
- Glaser A, Bürger S. Verification of fissile material cutoff treaty: the case of enrichment facilities and the role of ultra-trace level isotope ratio analysis. *J Radioanal Nucl Chem* 280:85–90; 2009.
- Gray DH, Ballard SC. EEG operational radiation surveillance of the WIPP Project during 2000. Carlsbad, NM: Environmental Evaluation Group; EEG-81 DOE/AL58309-81; 2001.
- Hamilton EI. Terrestrial radiation—an overview. *Radiat Phys Chem* 34:195–212; 1989.
- Hayes RB. An alternate error propagation approach. *Trans Amer Nucl Soc* 90:514–516; 2004.
- Huang WJ, Chen YH. Generalized skew-Cauchy distribution. *Statist Prob Lett* 77:1137–1147; 2007.
- Kenney JW, Downes PS, Gray DH, Ballard SC. Radionuclide baseline in soil near Project Gnome and the Waste Isolation Pilot Plant. Carlsbad, NM: Environmental Evaluation Group; EEG-58, DOE/AL/58309-58; 1995.
- Kenney JW, Gray DH, Ballard SC. Preoperational radiation surveillance of the WIPP project by EEG for the years 1993–1995. Carlsbad, NM: Environmental Evaluation Group; EEG-67, DOE/AL/58309-67; 1998.
- Kirchner TB, Webb JL, Webb SB, Arimoto R, Schoep DA, Steward BD. Variability in background levels of surface soil radionuclides in the vicinity of the U.S. DOE waste isolation pilot plant. *J Environ Radioact* 60:275–291; 2002.
- Knight FB. A characterization of the Cauchy type. *Proc Am Math Soc* 55:130–135; 1976.
- Kutschera W. Progress in isotope analysis at ultra-trace level by AMS. *Int J Mass Spectrom* 242:145–160; 2005.
- Liu T, Zhang P, Dai WS, Xie M. An intermediate distribution between Gaussian and Cauchy distributions. *Physica A* 391:5411–5421; 2012.
- Marsaglia G. Ratios of normal variables and ratios of sums of uniform variables. *J Amer Statist Assoc* 60:193–204; 1965.
- Meier-Augenstein W. Applied gas chromatography coupled to isotope ratio mass spectrometry. *J Chromatography A* 842:351–371; 1999.
- Minnema DM, Brewer LW. Background radiation measurements at the Waste Isolation Pilot Plant (WIPP) Site, Carlsbad, New Mexico. Albuquerque, NM: Sandia National Laboratory; SAND83-1296; 1983.
- NCI. Report on the feasibility of a study of the health consequences to the American population from nuclear weapons tests conducted by the United States and other nations. Vol 1 Technical Report. Washington, DC: Prepared for the U.S. Congress by the Department of Health and Human Services Centers for Disease Control and Prevention and the National Cancer Institute; 2005.
- National Council on Radiation Protection and Measurements. Environmental radiation measurements. Bethesda, MD: NCRP; Report No. 50; 1988.

- Orgill MM, Sehmel GA. Frequency and diurnal variation of dust storms in the contiguous USA. *Atmos Environ* 10:813–825; 1976.
- Patra AC, Mohapatra S, Sahoo SK, Tripathi RM, Puranik VD. Radioactive series disequilibria in underground uranium deposits of the Singhbhum Shear Zone, Eastern India. *J Radioanal Nucl Chem* 295:675–683; 2013.
- Placak OR. Nuclear explosions—peaceful applications. Las Vegas, NV: U.S. Public Health Service Off-Site Radiological Safety Organization; Project Gnome, Carlsbad, New Mexico Off-Site Radiological Safety Report; 1961.
- Rechard RP. Historical background on assessing the performance of the Waste Isolation Pilot Plant. Albuquerque, NM: Sandia National Laboratory; SAND98-2708; 1999.
- Stanley FE, Stalcup AM, Spitz HB. A brief introduction to analytical methods in nuclear forensics. *J Radioanal Nucl Chem* 295:1385–1393; 2013.
- Tandon L, Hastings E, Banar J, Barnes J, Beddingfield D, Decker D, Dyke J, Farr D, FitzPatrick J, Gallimore D (and 30 others). Nuclear, chemical and physical characterization of nuclear materials. *J Radioanal Nucl Chem* 276:467–473; 2008.
- United Nations Scientific Committee on the Effects of Atomic Radiation. Sources and effects of ionizing radiation. UNSCEAR 1993 Report to the General Assembly. New York: United Nations; 1993.
- U.S. Department of Energy. Waste Isolation Pilot Plant 1999 Site Environmental Report for 1998. Carlsbad, NM: U.S. DOE/WIPP 99-2225; 1999.
- U.S. Environmental Protection Agency. National emission standards for hazardous air pollutants. Washington DC: U.S. Environmental Protection Agency; 40 CFR 61; 2012.
- Vennard JK, Street RL. Elementary fluid mechanics. New York: John Wiley & Sons; 1975.
- Whicker JJ, Breshears DD, Wasiolek PT, Kirchner TB, Tavani RA, Schoep DA, Rodgers JC. Temporal and spatial variation of episodic wind erosion in unburned and burned semiarid shrubland. *J Environ Qual* 31:599–612; 2002.
- Whicker JJ, Pinder JE III, Breshears DD, Eberhart CF. From dust to dose: effects of forest disturbance on increased inhalation exposure. *Sci Total Environ* 368:519–530; 2006.
- WTS. Waste Isolation Pilot Plant documented safety analysis. Carlsbad, NM: Washington TRU Solutions LLC; DOE/WIPP 07-3372, Rev 3; 2011a.
- WTS. Mine ventilation rate monitoring annual report. Carlsbad, NM: U.S. Department of Energy; DOE/WIPP-11-3369; 2011b.
- X-5 Monte Carlo Team. MCNP—Monte Carlo N-particle transport code, version 5 volume 1: overview and theory. Los Alamos, NM: Los Alamos National Laboratory; LA-UR-03-1987; 2003.
- Ziskind G, Fichman M, Gutfinger C. Resuspension of particulates from surfaces to turbulent flows—review and analysis. *J Aerosol Sci* 26:613–644; 1995.

